Single-Molecule Study of an Adsorbed Oligonucleotide Undergoing Both Lateral Diffusion and Strong Adsorption

Mary J. Wirth* and Derrick J. Swinton

Department of Chemistry & Biochemistry, University of Delaware, Newark, Delaware 19716

Received: August 2, 2000; In Final Form: November 27, 2000

Single-molecule fluorescence spectroscopy was used to probe the lateral transport of an adsorbed oligonucleotide, the SP6 promoter primer, which is a 24-mer labeled at the 5′ end with tetramethylrhodamine. The oligonucleotide was adsorbed to the interface of an aqueous solution of 0.01 M KCl and silica chemically modified by chlorodimethyloctadecylsilane. Confocal fluorescence microscopy achieved single-molecule resolution, with a molecule in the beam 7% of the time. Autocorrelation of the data fit well to a model having two species, one diffusing and the other one undergoing transient strong adsorption. A small number of bursts, 0.3%, had unusually long durations, accounting for the slow component in the autocorrelation. When these long bursts were excised from the data, the autocorrelation fit well to simple diffusion, with $D = 4 \times 10^{-6}$ cm^2/s. Autocorrelation of the long bursts alone gave a rate constant for desorption of 3 s^{-1}. The strongly adsorbed molecules were found to comprise 10% of the total population of adsorbates. It is concluded that the lateral transport of the SP6 promoter primer is described by fast lateral diffusion interrupted by rare, reversible, strong adsorption to defect sites. During strong adsorption, the tetramethylrhodamine label undergoes hindered motion, suggesting it is not the adsorbing moiety.

Introduction

There has been a considerable amount of interest in the lateral diffusion of adsorbates at chemical interfaces for a variety of important systems, including biological membranes,[1] artificial membranes,[2,3] chromatographic interfaces,[4−8] and liquid−liquid interfaces.[9−11] Lateral diffusion is measured very accurately by either fluorescence recovery after photobleaching[4−8,12−14] or fluorescence correlation spectroscopy,[15−18] where the latter avoids perturbing the sample. The interpretation of the results is most straightforward when there is a single diffusing species; however, the data can, in principle, be analyzed for multiple species.[13,18]

Real systems can be complicated, and the correct interpretation can be crucial. For example, understanding the transport of oligonucleotides at chemical interfaces is essential to the design of new materials for rapid hybridization assays. Hybridization rates on planar surfaces have been shown to be limited by the lateral transport of oligonucleotides,[19,20] which is presumably controlled by the diffusion coefficient. However, real materials have strong adsorption sites, as demonstrated by decades of unsuccessful attempts by chromatographers to devise a material lacking such defect sites. In developing new materials that allow fast lateral diffusion, if the transport were unexpectedly slow, one would want to learn whether transport is limited by failure of the material to allow fast diffusion or by obstruction of transport due to strong adsorption to the defect sites. In fluorescence measurements of such transport, desorption from defect sites would contribute a decay component to the autocorrelation that might be difficult to distinguish from diffusion.

Single-molecule spectroscopy has been shown to provide information about the dynamics of individual oligonucleotide chains. Single-molecule fluorescence spectroscopy provides a means of distinguishing diffusing molecules from specifically adsorbed molecules. The basis for this distinction is that, to a first approximation, the count rate, I, is dependent upon the radial position, r, of the molecule in the beam, as described by eq 1.

$$I_r = I_0 \exp(-r^2/2s^2) \tag{1}$$

The count rate of diffusing molecules fluctuates because r fluctuates, while the count rate of strongly adsorbed molecules remains constant. We studied single molecules of DiI at a chromatographic interface and observed many long bursts that had a constant count rate within the shot noise.[21] Strong adsorption of DiI was observed to occur for approximately 1% of the molecules entering the beam, with an average duration of 100 ms. Strong adsorption was subsequently attributed to hydrogen-bonding to silanols on the silica substrate because reduced exposure of the silica substrate reduced strong adsorption.[22]

Oligonucleotides are designed by nature to hydrogen bond. Observation of single oligonucleotide chains, labeled with tetramethylrhodamine, has been demonstrated as a means of probing heterogeneous dynamics.[23,24] The ability of single-molecule spectroscopy to resolve radial trajectories of each species as it passes through the beam enables one to test whether lateral transport of labeled oligonucleotides can be complicated by strong adsorption to silanols. The purpose of this work is to investigate the lateral transport of single molecules of the SP6 promoter primer, a 24-mer, labeled with tetramethylrhodamine, at the interface of water and silica modified with chlorodimethyloctadecylsilane. This surface was chosen because it is the stationary phase of choice for analysis and purification of labeled oligonucleotides by HPLC, making it a candidate for hybridization assays.

* To whom correspondence should be addressed.

10.1021/jp0027647 CCC: $20.00
Published on Web 01/25/2001

Experimental Section

The experimental apparatus was identical to one we previously used,[21] where an inverted optical microscope (Zeiss Axiovert 100) was used in combination with an external confocal pinhole to allow single-molecule measurements with a high fluorescence-to-background ratio. A 100 μW beam from a mode-locked argon ion laser (Coherent, Inc.), operated at 514.5 nm, was focused at the interface using a 100× oil immersion objective (NA = 1.40). The beam size at the focus was evaluated using a CCD camera (Roper Instruments, TEK512B) and a surface having a high concentration of oligonucleotide. A ronchi ruling was subsequently placed in the object plane to calibrate the spatial scale of the CCD. The size of the confocal pinhole was 25 μm, chosen to encircle the image of the Gaussian beam over $\pm 2\sigma$. The pinhole image was refocused onto an actively quenched avalanche photodiode (EG&G Optoelectronics), and its output was time-filtered (Oxford-Tennelec TAC 480) to eliminate signal caused by Raman scattering from the solvent. Laser power was varied to ensure that photobleaching and optical trapping were negligible, and the average power in the experiments was 2 μW. Burst data were collected for 65 s using a 4 ms dwell time and 16 384 channels in the multichannel scalar (Oxford-Tennelec). The data were analyzed using Origin to autocorrelate the burst data and Matlab for programming to evaluate individual burst characteristics.

A fused silica microscope slide (ESCO) was derivatized with chlorodimethyloctadecylsilane in dry toluene for 3 h, using pyridine as a catalyst, and then rinsed to cleanliness. This procedure gives full surface coverage of the silane to the steric limit determined by the methyl side groups of the silicon atom.[8] The SP6 promoter primer, obtained from New England Biolabs, was dissolved in 0.01 M KCl, diluted to nanomolar levels, and then equilibrated with the surface. The interface was placed in the focal plane of the microscope, and the fluorescence was monitored as the solution was successively diluted until the concentration decreased to one molecule in the beam <10% of the time.

Results and Discussion

For a sample of adsorbed SP6 promoter primer in contact with a 0.01 M solution of KCl, where the surface concentration was diluted to a single-molecule level, burst data of 80 000 points were acquired with a 4 ms dwell time. The data were autocorrelated, and the resulting decay is plotted in Figure 1, where a log scale for the time axis is used to accentuate the details of the early part of the decay. The theoretical autocorrelation decay for a single laterally diffusing species is given by eq 2, where D is the lateral diffusion coefficient and s^2 is the beam variance.[15]

$$G(\tau) = A/(1 + D\tau/s^2) + B \qquad (2)$$

The best fit of eq 2 to the autocorrelation decay is shown in Figure 1, with $D = 2 \times 10^{-7}$ cm^2/s. The fit is poor, indicating that the lateral transport is not described by simple diffusion. Equation 2 was derived for the case of a Gaussian beam,[15] so beam distortion is a possible cause of the poor fit. However, Figure 2 shows a representative cross-section of the beam profile and an excellent best fit to a Gaussian of $s = 0.85$ μm. Therefore, the disagreement between the autocorrelation decay and eq 2 cannot be attributed to beam distortion.

A second possible cause of the deviation of the decay from eq 1 is that the diffusion of the SP6 promoter primer is complicated by multiple conformations, which can arise from

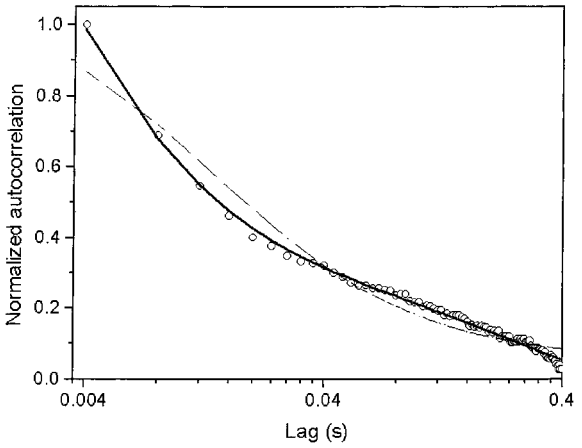

Figure 1. Autocorrelation decay (○), best fit to a single diffusing species of $D = 5 \times 10^{-7}$ cm^2/s (---), and best fit to two diffusing species of $D_1 = 2 \times 10^{-8}$ and $D_2 = 2 \times 10^{-6}$ cm^2/s (—). The dashed line coincides with the best fit of a single diffusing species having $D = 4 \times 10^{-6}$ cm^2/s plus an exponential decay of $\tau = 0.3$ s.

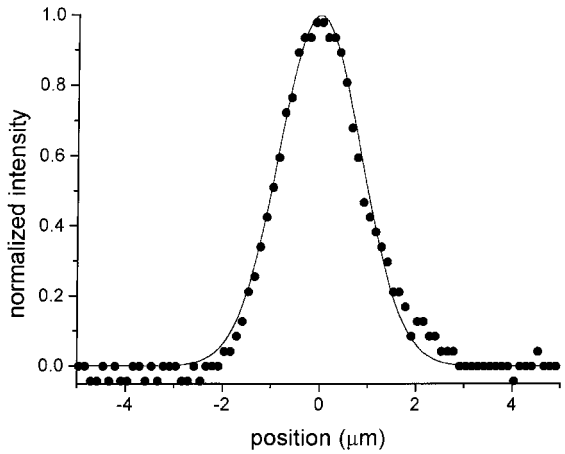

Figure 2. Cross-section of the beam profile (●) and best fit to a Gaussian function having a standard deviation of 0.85 μm (—).

self-hybridization, where complementary sequences on opposites sides of the oligonucleotide pair with one another. The SP6 sequence (5′-R6G-CATACGATTTAGGTGACACTATAG) allows for self-hybridization at the underlined sequences, as well as other weaker self-hybridized structures. The autocorrelation decay for multiple species has been shown to be simply the sum of decays for individual species, provided that the different species diffuse independently of one another.[18] The function is given in eq 3.

$$G(\tau) = \sum_i A_i/(1 + D_i\tau/s^2) + B \qquad (3)$$

Figure 1 shows the best fit of the autocorrelation decay to eq 3 for two diffusing species. The fit is excellent, and the two diffusion coefficients are $D_1 = 2 \times 10^{-8}$ and $D_2 = 2 \times 10^{-6}$ cm^2/s. On mathematical grounds alone, the interpretation of two diffusing species cannot be rejected. However, on chemical grounds, it seems unreasonable for different conformations of the same species to have diffusion coefficients that differ by 2 orders of magnitude. The Debye−Stokes relation, given in eq 4, predicts that the diffusion coefficient scales inversely with the geometric mean, a, of the three molecular axes, where η is the microviscosity.

$$D = kT/6\pi\eta a \qquad (4)$$

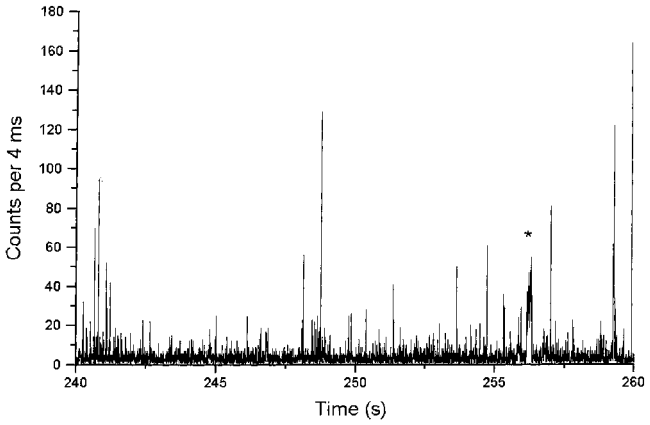

Figure 3. A 20 s segment of the burst data, plotted as counts per 4 ms bin vs time. The asterisk denotes an unusually long burst.

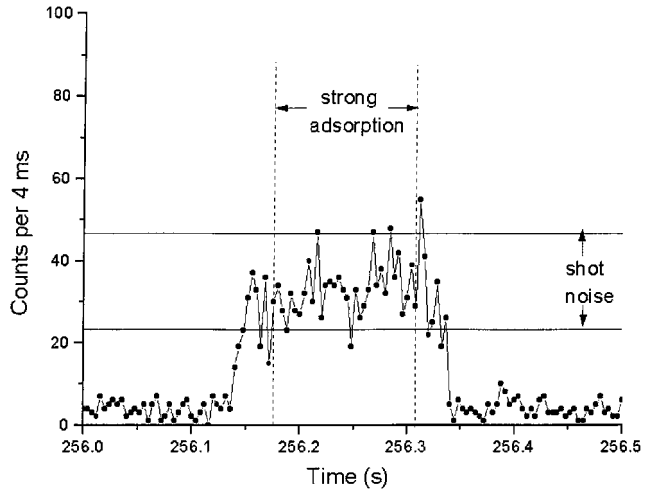

Figure 4. Unusually long burst of Figure 3 on an expanded scale of 0.5 s. The solid lines show the shot noise level over $\pm 2\sigma$ about the average. The dotted lines provide an estimate for the time span over which the count rate is constant, which indicates strong adsorption.

There would have to be a 100-fold change in a to explain the disparate diffusion coefficients. A systematic study of the relation between diffusion coefficient and oligonucleotide conformation has not been reported, but it does not seem reasonable that self-hybridization would change the effective size of the oligonucleotide by a factor of 100. Other possibilities must be considered.

A third possible cause of the deviation of the behavior from simple diffusion is that transient strong adsorption could distort the autocorrelation. To evaluate the possibility that strong adsorption of the SP6 promoter primer causes the deviation of the autocorrelation from eq 1, we employ single-molecule resolution to examine individual bursts. Figure 3 shows a subset of the raw fluorescence data over a 20 s interval. The sharp fluctuations in fluorescence count rate are due to the rapid Brownian motion of molecules through the focused Gaussian beam. In Figure 3, the asterisk denotes an unusually long burst, and Figure 4 shows this same long burst on an expanded scale. The burst has a lengthy interval where the count rate remains nearly constant, usually within the shot noise; therefore, this behavior is consistent with strong adsorption. The shot noise indicated in the graph of Figure 4 corresponds to the 95% confidence level. The graph shows an estimate for the duration of strong adsorption, which is 130 ms. The constant count rate over the 130 ms period within the long burst of Figure 4 is thus consistent with a strong adsorption event.

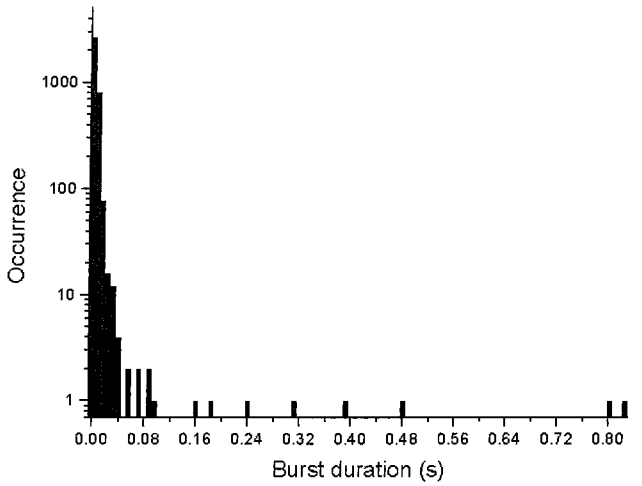

Figure 5. Histogram of the durations of the bursts. The burst duration was measured as the elapsed time that the fluorescence count rate remained above the threshold of 9 counts/4 ms.

To extract quantitative information about strong adsorption requires that single-molecule events are resolved. Poisson statistics allow calculation of the probability of having single vs multiple molecules in the beam, and a detailed statistical analysis is essential for interpretation of single-molecule behavior.[25−27] Analysis of the data reveals that the signal exceeds a threshold value of 9 counts/4 ms for 5672 out of 80 000 channels. The background is 3 counts/4 ms, and the probability of shot noise on the background reaching the threshold of 9 is calculated from the probability, P, of observing x events if the average observation rate is μ.

$$P(x) = (\mu^x/x!)\exp(-\mu) \tag{5}$$

From the background count rate of $\mu = 3$, the probability of the shot noise reaching the threshold of 9 is $\{P(9) + P(10) + ... + P(\infty)\} = 0.0038$; therefore, 304 bursts out of the 80 000 channels are due to shot noise on the background. One cannot identify these, except to say they are a subset of the bursts that are a single channel in duration. After the 304 bursts due to shot noise are subtracted, there are 5368 channels, out of 80 000 channels, that are attributable to fluorescence of diffusing SP6 molecules. This gives an average observation rate of 7%. The probability of having two molecules in the beam simultaneously is calculated from eq 5 to be 0.2% for $\mu = 5368/80\,000$. Therefore, of the 5368 channels above threshold due to signal, an estimate of 11 bursts would be due to two molecules being in the beam simultaneously, and this must be considered in the interpretation of the transient signals. A total of 3662 bursts were counted, and after the 304 bursts attributable to shot noise in the background are subtracted, this leaves 3358 times that a molecule entered the beam over the 80 000 channels. Therefore, the average time between bursts is 95 ms. It can be concluded that the burst data are overwhelmingly due to single-molecule events.

A histogram of burst durations is shown in Figure 5. Due to the enormous fraction of short bursts, the frequency of occurrence is plotted on a log scale. Figure 5 illustrates that the vast majority of the bursts are significantly shorter than the average 95 ms between bursts, underscoring the fact that single-molecule events are resolved. The histogram reveals a small population of bursts whose durations are long compared to those of the vast majority of bursts. The durations of these long bursts range from 160 to 800 ms. We performed simulations of Brownian motion and found that no such tail in the histogram of burst

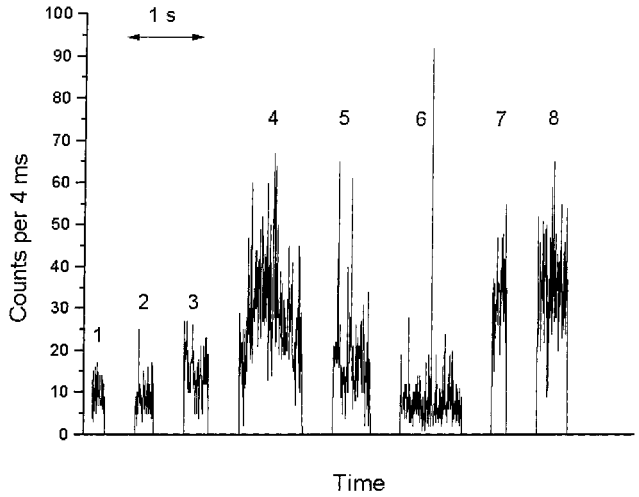

Figure 6. Count rate vs time for bursts longer than 0.1 s in duration. These signals have been extracted from the data set and are plotted artificially as a train. The time scale is indicated in the upper left of the figure. The bursts are numbered to correspond to the discussion in the text.

durations would appear if there were a single diffusing species. The long bursts are attributed to either a slowly diffusing second species or to strong adsorption of the same species that is undergoing rapid diffusion. Their durations exceed the 95 ms average duration between bursts; therefore, multiple molecules are likely to be in the beam during these long bursts.

The data for the eight longest bursts from the histogram of Figure 5 are plotted artificially as a train of bursts in Figure 6. Each high spike in the bursts labeled 2, 5, and 6 is likely due to an additional molecule diffusing through the beam, which is expected for these long bursts. Burst 7 is the same one shown in Figure 4, where the count rate is consistent with the stationary radial position of the molecule for most of the duration of the burst. The bursts labeled 1, 2, 6, and 8 have count rates that are close to remaining within the shot noise for most of the duration of the bursts. These could be attributed to strong adsorption if the additional fluctuation can be explained. The downward spike most evident in burst 8, but also evident in bursts 3−5, could be due to blinking, which is known to occur for rhodamine dyes.[26−31] Blinking is a transient loss of fluorescence for a single molecule while it is trapped in its lowest triplet state, making it invisible in a fluorescence experiment until the molecule relaxes back to its ground state. Aside from the apparent blinking and multiple-molecule events, there still remains a significant amount of fluctuation in the intensity. Bursts 4 and 5 show the most variation in count rate, and they are among the longest bursts.

All of the long bursts for SP6 show more intensity fluctuations than did comparably long bursts for DiI. For example, Figure 7 shows a comparison of long bursts for DiI and for SP6 at the same interface. For DiI, the count rate remains within the shot noise over the time period from 47.6 to 47.8 s. For SP6, the average count rate continually drifts over time, well outside the shot noise, for this burst. The frequent observation that the count rate for long bursts of SP6 fluctuates well outside the shot noise raises the question of whether these long bursts are due to strong adsorption or to a slowly diffusing species.

If the long bursts of SP6 were due to slow diffusion, the autocorrelation of the set of long bursts would fit eq 2. If the long bursts were due to strong adsorption, the autocorrelation would fit an exponential decay, assuming there is a single type of strong adsorption site. Figure 8 shows a plot of the autocorrelation of the long bursts, compared to the best fit for pure diffusion, as described by eq 2, and the best fit for an exponential decay. The autocorrelation fits much better to an exponential decay, establishing that the long bursts are attributable to strong adsorption, not to a slowly diffusing species. The decay constant is 0.3 s, although the best fit is not excellent. Eight bursts would not be enough to give an excellent fit to an exponential decay. The finite size of the data set introduces a linear functionality to the decay, evident in Figure 8, because the autocorrelation of a top-hat function is a linear decay. Also, the inability to resolve strong adsorption events shorter than 0.1 s reduces the steepness of the decay that an exponential function would have at earlier times. If the long bursts were due to a slow diffusion species, the initial part of the decay would sharply drop in accordance with eq 2 despite the absence of the bursts shorter than 0.1 s. This is because Brownian motion would give more fluctuation than the long bursts exhibit. It is concluded that the long bursts of SP6 are due to strong adsorption.

It is chemically reasonable that strongly adsorbed oligonucleotides would have fluorescence fluctuations outside the shot noise. When the oligonucleotide is strongly adsorbed to the surface, the rhodamine label could change in orientation or in environment despite the overall molecule remaining stationary with respect to radial position in the Gaussian beam. The rhodamine is tethered to the oligonucleotide, so it does not necessarily experience the same deep potential well if a site on the oligonucleotide is responsible for strong adsorption. The tethered rhodamine could change positions on the molecular scale, which could change the fluorescence intensity through either a spectral shift or a rotation of the transition moment. Further experiments are needed for elucidation. For the intensity fluctuations to occur on the time scale of tens to hundreds of milliseconds, the motions of the rhodamine label would have to occur on this time scale, suggesting that the label often encounters shallow potential wells during strong adsorption of the oligonucleotide. For single DiI molecules, occasionally discrete jumps in count rate were observed for the water/C_{18} interface,[21] and a jump in the emission spectrum was observed for a dry poly(methyl methacrylate) film.[28] The more constant count rate for strongly adsorbed DiI, compared to SP6, at the chromatographic interface is likely due to the fact that the DiI chromophore itself is specifically adsorbed, rather than being tethered to the specifically adsorbing moiety. One practical consequence for studies of fluorescence-labeled oligonucleotides is that strong adsorption events for single molecules cannot be identified by a constant count rate. In this work, their identification relies upon the functionality of the autocorrelation decay.

It is concluded that the long bursts are due to strong adsorption of the SP6 molecules to the surface. Such strong adsorption is consistent with the behavior observed universally for hydrogen-bonding species in HPLC, including organic bases, peptides, and proteins.[32−35] This phenomenon gives rise to the ubiquitous peak tailing of hydrogen-bonding species. It is speculated, on the basis of this wealth of literature for chromatographic tailing, that the strong adsorption of the SP6 promoter primer occurs through hydrogen-bonding of one or more of the bases to the exposed surface silanols. It has been shown that the phosphate groups of oligonucleotides adsorb to bare silica through hydrogen-bonding to silanols, despite the charge repulsion.[36] It is also possible that the label itself adsorbs, although the fact that the bursts fluctuate outside the shot noise suggests that the label is remote from the site of adsorption. Further work is needed to establish definitively how the

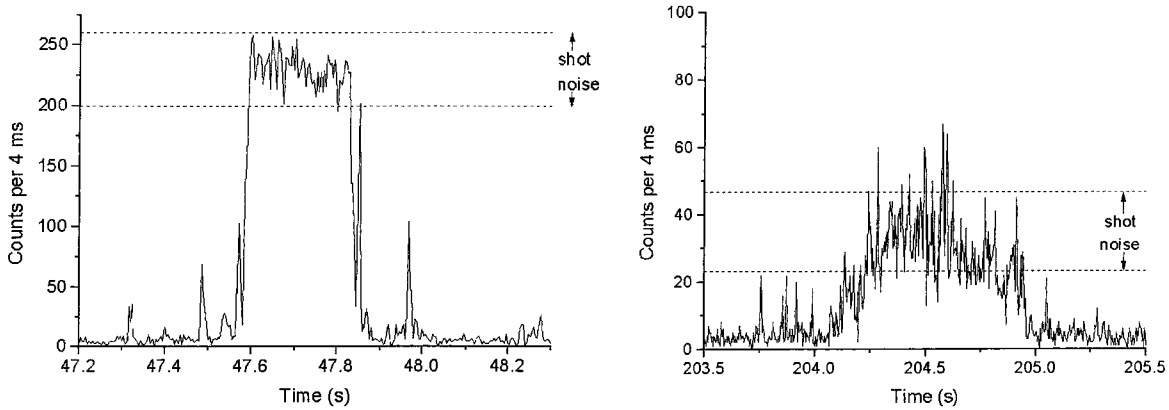

Figure 7. Comparison of long bursts for DiI (left) and SP6 (right). This illustrates the contrast in behavior between DiI, which has a level count rate, and SP6, which has a fluctuating count rate.

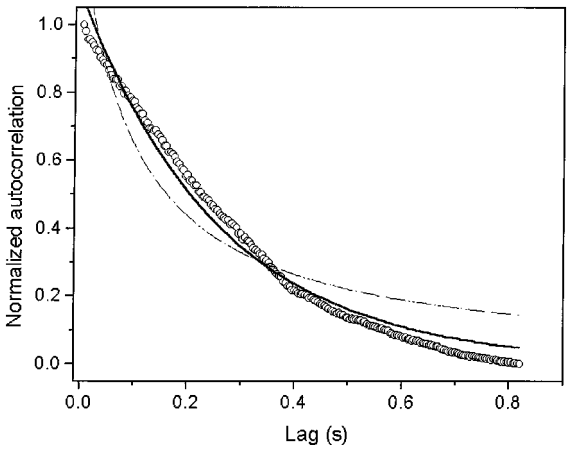

Figure 8. Normalized autocorrelation decay for the long bursts alone (○). Also shown are the best fit to eq 2 for simple diffusion (− · −), where $D = 2 \times 10^{-5}$ cm^2/s, and the best fit to an exponential decay (−), where the decay constant is 0.3 s.

oligonucleotide attaches, and it is possible that there are multiple ways.

The long bursts due to strong adsorption have a distribution of durations that is described by the desorption rate. Since the concentration at the interface remains constant throughout the experiment, desorption means leaving a strong adsorption site to begin diffusing at the interface again. Desorption is typically an activated first-order decay process. If there were a single type of strong adsorption site, with k_d as the rate constant for desorption, the desorption rate would depend on the concentration of SP6 molecules on the strong adsorption sites, which is Γ_S.

$$-d\Gamma_s/dt = k_d\Gamma_s \tag{6}$$

Therefore, for an ensemble of specifically adsorbed oligonucleotides that is described by a single value of k_d, the concentration of adsorbates decays exponentially.

$$\Gamma_s(t) = \Gamma_s(0)\exp(-k_d t) \tag{7}$$

In the single-molecule experiment, the probability of a molecule remaining adsorbed would decrease with time as described by this exponential decay. For the eight long bursts, the average duration is calculated to be $1/k_d = 0.3$ s, in agreement with the decay constant for the autocorrelation of the eight long bursts.

The autocorrelation decay of the full set of burst data can now be tested to determine whether it can be explained by the two processes of diffusion and strong adsorption. Since these two processes are statistically independent, the autocorrelation would be the sum of two autocorrelations, where A and $1 - A$ are proportional to the number of molecules undergoing the respective processes.

$$A/(1 + Dt/s^2) + (1 - A)\exp(-k_d t) + B \tag{8}$$

The best fit of eq 8 to the autocorrelation of the burst data is identical to that of the dashed line illustrated in Figure 1, which was for two diffusing species, and the best fit reveals $k_d = (0.3\ \text{s})^{-1}$. This desorption rate constant is in excellent agreement with the average duration of long bursts and the decay constant for the autocorrelation of the long bursts, both of which were found to be 0.3 s. The agreement among these calculations of k_d supports the assumption of nearly homogeneous strong adsorption, and it further supports the interpretation that the long bursts are due to strong adsorption, not slow diffusion. The best fit further reports $D = 4 \times 10^{-6}$ cm^2/s.

The probability of strong adsorption is very low, 8 events out of 3358 bursts, or 0.3(±0.2)% for the 0.85^2 μm^2 beam variance. Strong adsorption is thus a rare event. The total number of channels over which molecules are specifically adsorbed is 771 channels out of the total 5368 channels above background, which means that, 14(±7)% of the total time that a molecule is being detected, a molecule is specifically adsorbed. Since a time average and an ensemble average are equivalent for a large data set, the relative total times for adsorption and diffusion should correspond to the coefficients A and $1 - A$ in eq 8. The best fit of the autocorrelation of the total data set to eq 8 reported $A = 0.90$; therefore, the fraction adsorbed is estimated to be 10%, assuming that the diffusing and adsorbed species have equal molar absorptivities and fluorescence quantum yields. This is in reasonable agreement with the 14% obtained from the total time of strong adsorption of single molecules. This agreement between the single-molecule counting and the autocorrelation, to calculate the fraction strongly adsorbed, lends further support to the interpretation that the oligonucleotide undergoes a combination of fast diffusion and rare, strong adsorption.

The experiment reveals that strong adsorption itself is a rare process; however, the population of specifically adsorbed molecules is plentiful. In other words, despite the adsorption probability of <1%, specifically adsorbed molecules account for approximately 10% of the adsorbed molecules. The reason that an improbable process can create a significant equilibrium population is that the desorption rate is slow, allowing strongly adsorbed molecules to accumulate. This was the same circumstance as that reported for DiI, where it was explained that a

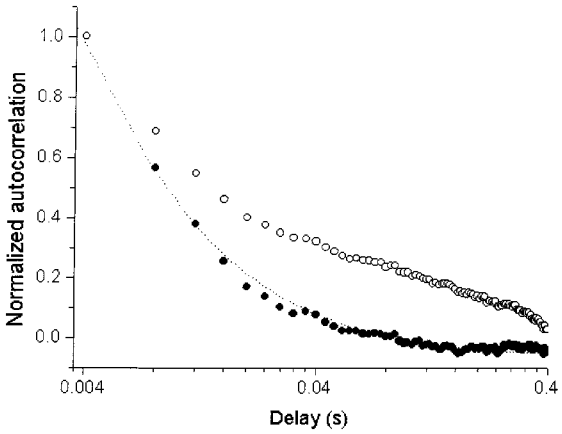

Figure 9. Normalized autocorrelation of the burst data after the eight long bursts have been removed from the data set (●) and best fit of this decay to eq 2 for simple diffusion (---), which gives $D = 4 \times 10^{-6}$ cm^2/s. For comparison, the normalized autocorrelation of the full data set is shown (○).

combination of low adsorption probability and even lower desorption probability is what underlies chromatographic tailing.[21]

Single-molecule spectroscopy uniquely allows one to examine how the autocorrelation would appear if the specific adsorption events did not occur. The long bursts can easily be excised from the total set of burst data and separately autocorrelated. Figure 9 shows a comparison of the original autocorrelation and the autocorrelation of only the bursts that are less than 0.1 s in duration. The best fit of the new autocorrelation is to eq 2, which describes the diffusion of a single species, and the diffusion coefficient is 4×10^{-6} cm^2/s, in agreement with the value determined by autocorrelation of the full data set and analysis by eq 8. This confirms that the long bursts cause the deviation of the autocorrelation from simple diffusion. The diffusion coefficient is comparable to diffusion coefficients of interfacial dye molecules that are not attached to 24-mers,[8,21] and the value is much faster than the diffusion coefficient of rubrene at the same interface.[6] It is interesting to speculate why the labeled SP6 oligonucleotide would diffuse faster than these molecules that are much smaller. It is possible that the lower hydrophobicity of the oligonucleotide reduces its interaction with the hydrocarbon monolayer, which is known to be viscous.[4,38]

Conclusions

The ability to resolve single molecules is essential to confident interpretation of the lateral transport of the SP6 oligonucleotide. Fluorescence correlation spectroscopy cannot distinguish the cases of two disparate diffusing species vs one species undergoing diffusion and strong adsorption. Single-molecule spectroscopy is unique in its capability to distinguish these two cases because bursts from strong adsorption events can be isolated from the data set and examined separately.

The SP6 oligonucleotide undergoes both very fast lateral diffusion and rare, reversible, strong adsorption at the interface of water and a monolayer of hydrocarbon on silica. The desorption rate constant is 3 s^{-1}. Strong adsorption occurs with a probability of only 0.3% in this experiment. The low desorption rate gives rise to a population of strong adsorbates that is estimated to be 10% of the total population of adsorbed oligonucleotide, in the limit of low concentration of oligonucleotide.

For transport of the oligonucleotide through a channel in contact with the surface, such as for chromatography or electrophoresis, the zone would tail due to the rare, strong adsorption. Assuming that the label is not the cause of strong adsorption, the results have ramifications for hybridization. Oligonucleotides captured by this surface would undergo fast diffusion that would facilitate hybridization. The strong adsorption would lower the hybridization rate by about 10%, assuming the rate is diffusion limited.

Acknowledgment. This work was supported by the National Science Foundation under Grant CHE-0078847. D.J.S. is grateful to the University of Delaware for a Presidential Fellowship.

References and Notes

(1) Greenberg, M. L.; Axelrod, D. *J. Membr. Biol*. **1993**, *131*, 115−127.
(2) Ong, S. W.; Qiu, X. X.; Pidgeon, C. *J. Phys. Chem.* **1994**, *98*, 10189−10199.
(3) Schutz, G. J.; Schindler, H.; Schmidt, T. *Biophys. J.* **1997**, *73*, 1073−1080.
(4) Hansen, R. L.; Harris, J. M. *Anal. Chem*. **1995**, *67*, 492−498.
(5) Kovaleski, J. M.; Wirth, M. J. *J. Phys. Chem. B* **1996**, *100*, 10304−10309.
(6) Hansen, R. L.; Harris, J. M. *Anal. Chem*. **1996**, *68*, 2879−2884.
(7) Zulli, S. L.; Kovaleski, J. M.; Zhu, X. R.; Harris, J. M.; Wirth, M. J. *Anal. Chem*. **1994**, *66*, 1708−1712.
(8) Kovaleski, J. M.; Wirth, M. J. *J. Phys. Chem. B* **1997**, *101*, 5545−5548.
(9) Kovaleski, J. M.; Wirth, M. J. *J. Phys. Chem*. **1995**, *99*, 4091−4095.
(10) Wirth, M. J.; Burbage, J. D. *J. Phys. Chem.* **1992**, *96*, 9022−9025.
(11) Murad, M. M. *J. Fluoresc.* **1999**, *9*, 257−263.
(12) Axelrod, D.; Koppel, D. E.; Schlessinger, J.; Elson, E.; Webb, W. W. *Biophys. J*. **1976**, *16*, 1055−1069.
(13) Gordon, G. W.; Chazotte, B.; Wang, X. F.; Herman, B. *Biophys. J.* **1995**, *68*, 766−778.
(14) Kovaleski, J. M.; Wirth, M. J. *Anal. Chem*. **1997**, *69*, A600−A605.
(15) Elson, E. L.; Magde, D. *Biopolymers* **1974**, *13*, 1−27.
(16) Magde, D.; Elson, E. L.; Webb, W. W. *Biopolymers* **1974**, *13*, 29−61.
(17) Magde, D. *Q. Rev. Biophys.* **1976**, *9*, 35−47.
(18) Meseth, U.; Wohland, T.; Rigler, R.; Vogel, H. *Biophys. J.* **1999**, *76*, 1619−1631.
(19) Wang, D.; Gou, Shi-Yuan.; Axelrod, D. *Biophys. Chem*. **1992**, *43*, 117−137.
(20) Chan, V.; Graves, D. J.; McKenzie, S. E. *Biophys. J*. **1995**, *69*, 2243−55.
(21) Wirth, M. J.; Swinton, D. J. *Anal. Chem.* **1998**, *70*, 5264−5271.
(22) Wirth, M. J.; Ludes, M. D.; Swinton, D. J. *Anal. Chem*. **1999**, *71*, 3911−3917.
(23) Wennmalm, S.; Edman, L.; Rigler, R. *Chem. Phys*. **1999**, *247*, 61−67.
(24) Edman, L.; Mets, U.; Rigler, R. *Proc. Natl. Acad. Sci. U.S.A.* **1996**, *93*, 6710−6715.
(25) Fister, J. C.; Jacobson, S. C.; Davis, L. M.; Ramsey, J. M. *Anal. Chem*. **1998**, *70*, 431−437.
(26) Lermer, N.; Barnes, M. D.; Kung, C. Y.; Whitten, W. B.; Ramsey, J. M. *Anal. Chem*. **1997**, *69*, 2115−2121.
(27) Chen, D. Y.; Dovichi, N. J. *Anal. Chem*. **1996**, *68*, 690−696.
(28) Trautman, J. K.; Macklin, J. J. *Chem. Phys. Lett*. **1996**, *205*, 221−229.
(29) Dickson, R. M.; Cubitt, A. B.; Tsien, R. Y.; Moerner, W. E. *Nature* **1997**, *388*, 355−358.
(30) Jung, G.; Wiehler, J.; Gohde, W.; Tittel, J.; Basche, T.; Steipe, B.; Brauchle, C. *Bioimaging* **1998**, *6*, 54−61.
(31) Sauer, M.; Drexhage, K. H.; Liebewirth, U.; Muller, R.; Nord S.; Zander, C. *Chem. Phys. Lett.* **1998**, *284*, 153−163.
(32) Kohler, J.; Kirkland, J. J. *J. Chromatgr*. **1987**, *385*, 125−150.
(33) Cox, G. B. *J. Chromatgr., A* **1993**, *656*, 353−367.
(34) McCalley, D. V. *J. Chromatgr., A* **1994,** *664*, 139−147.
(35) Nawrocki, J.*J. Chromatgr., A* **1997**, *779*, 29−71.
(36) Mao, Y.; Daniel, L.; Whittaker, N.; Saffioti, U. *Environ. Health Perspect.* **1994**, *102*, 165−171.
(37) Ellison, E. H.; Marshall, D. B. *J. Phys. Chem*. **1991**, *95*, 808−813.